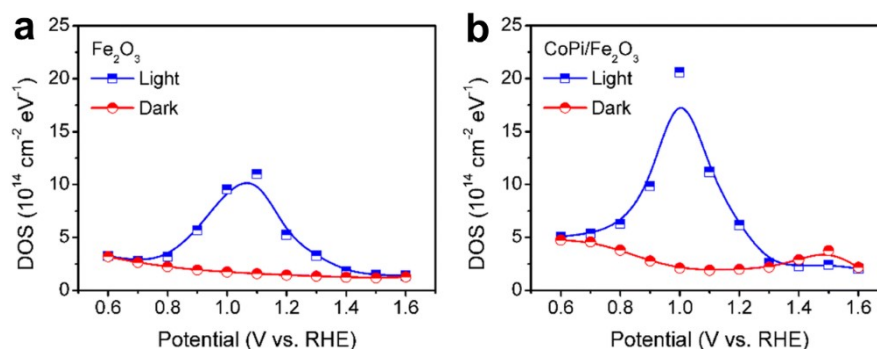
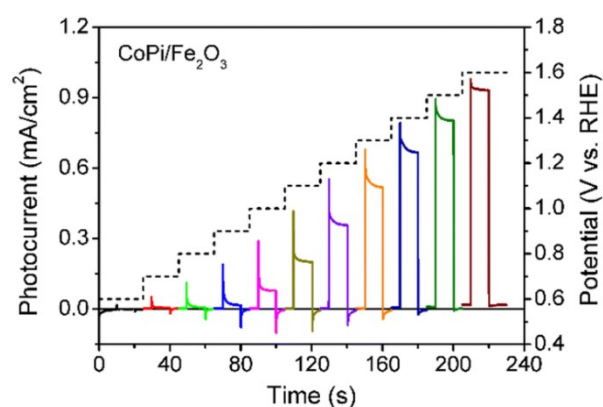


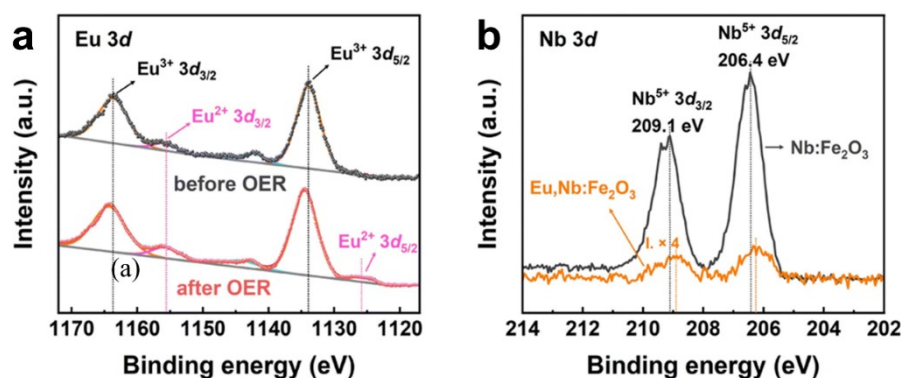
## Supplementary Figures



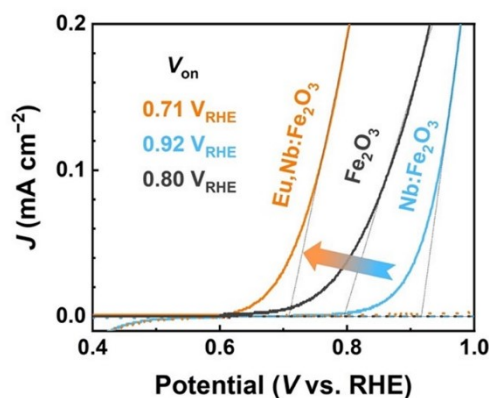
**Supplementary Fig. 1** DOS of surface states in (a) bare  $\text{Fe}_2\text{O}_3$  and (b)  $\text{CoPi}/\text{Fe}_2\text{O}_3$  as a function of potential under illumination (456 nm LED:  $5 \text{ mW cm}^{-2}$ ) and in the dark. Reprinted with permission from ref.23. Copyright 2023 Royal Society of Chemistry.



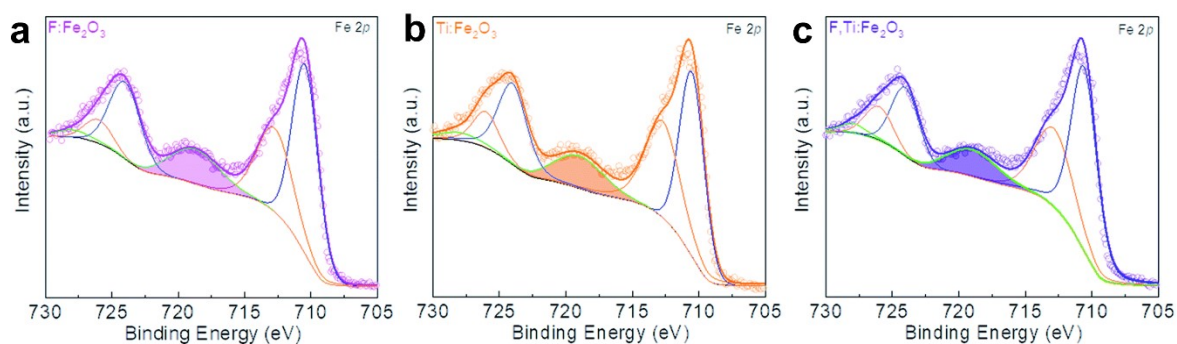
**Supplementary Fig. 2**  $\text{CoPi}/\text{Fe}_2\text{O}_3$  photoanodes under chopped illumination (AM 1.5 G:  $100 \text{ mW cm}^{-2}$ ). Reprinted with permission from ref.23. Copyright 2023 Royal Society of Chemistry.



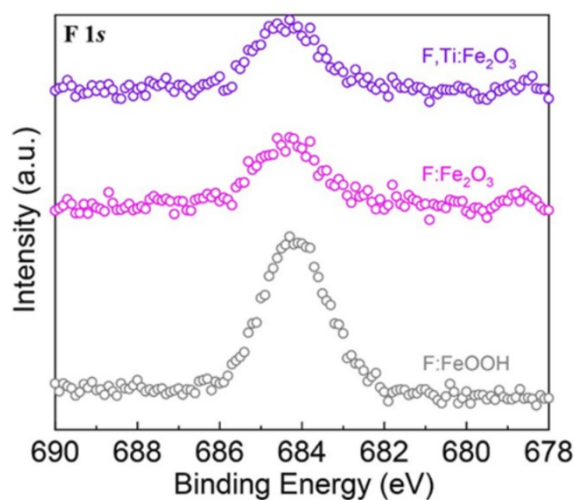
**Supplementary Fig. 3** (a) Eu  $3d$  XPS spectra of  $\text{Eu,Nb} : \text{Fe}_2\text{O}_3$  before and after the OER, (b) Nb  $3d$  XPS spectra of  $\text{Nb} : \text{Fe}_2\text{O}_3$  and  $\text{Eu,Nb} : \text{Fe}_2\text{O}_3$ . Reprinted with permission from ref.25. Copyright 2024 Royal Society of Chemistry.



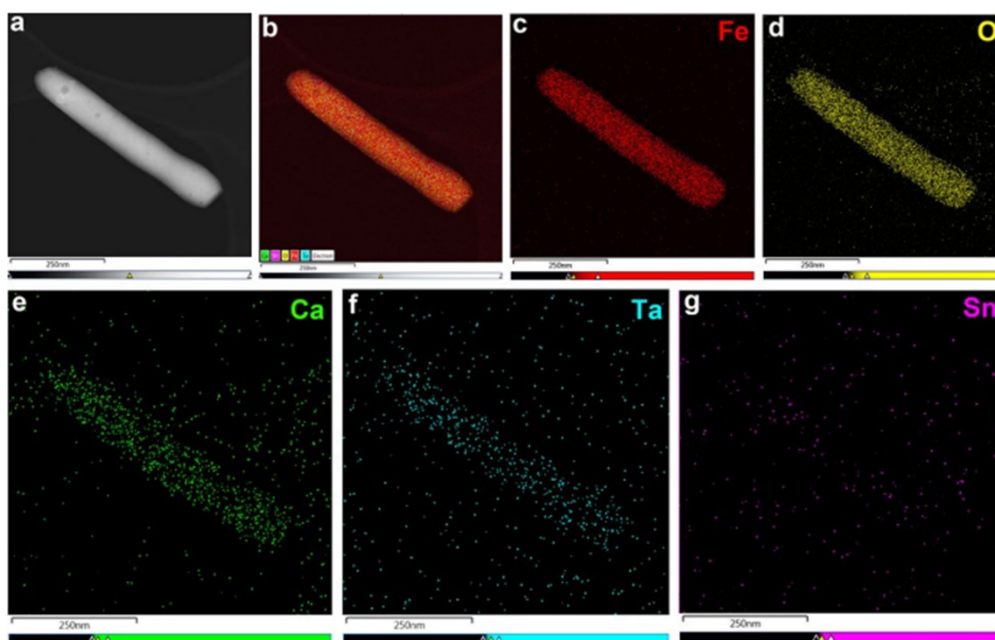
**Supplementary Fig. 4** Extracted  $V_{on}$  of  $\text{Fe}_2\text{O}_3$ ,  $\text{Nb} : \text{Fe}_2\text{O}_3$  and  $\text{Eu,Nb} : \text{Fe}_2\text{O}_3$ . Reprinted with permission from ref.25. Copyright 2024 Royal Society of Chemistry.



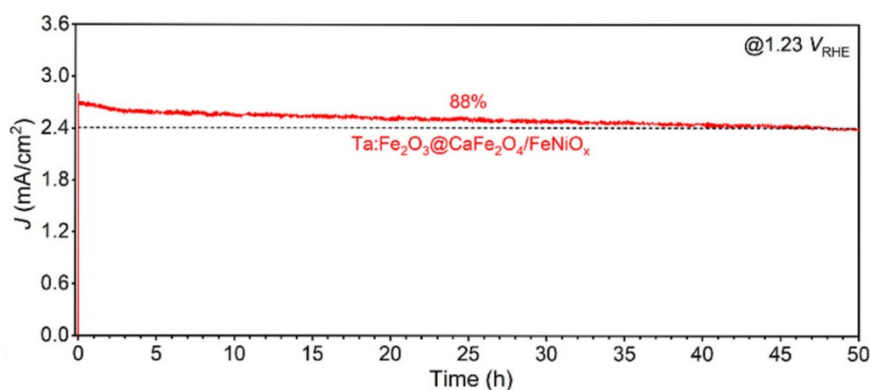
**Supplementary Fig. 5** Fe 2p XPS spectra of (a)  $\text{F}:\text{Fe}_2\text{O}_3$ , (b)  $\text{Ti}:\text{Fe}_2\text{O}_3$ , and (c)  $\text{F,Ti}:\text{Fe}_2\text{O}_3$ . The coloured peaks denote the  $\text{Fe}^{3+}$  satellite peak. Reprinted with permission from ref.26. Copyright 2022 Royal Society of Chemistry.



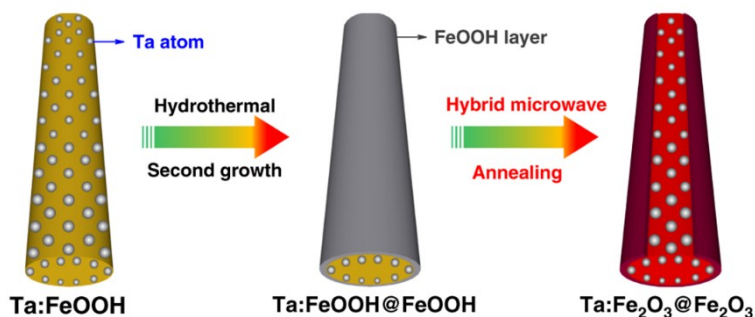
**Supplementary Fig. 6** F 1s XPS spectra of  $\text{F}:\text{FeOOH}$ ,  $\text{F}:\text{Fe}_2\text{O}_3$  and  $\text{F,Ti}:\text{Fe}_2\text{O}_3$ . Reprinted with permission from ref.26. Copyright 2022 Royal Society of Chemistry.



**Supplementary Fig. 7** HAADF (a) and element mapping of Ta:Fe<sub>2</sub>O<sub>3</sub>@CaFe<sub>2</sub>O<sub>4</sub> nanorod (b, all elements. c, Fe. d, O. e, Ca. f, Ta. g, Sn). Reprinted with permission from ref.27. Copyright 2023 American Chemical Society.



**Supplementary Fig. 8** The long-term stability of Ta:Fe<sub>2</sub>O<sub>3</sub>@CaFe<sub>2</sub>O<sub>4</sub>/FeNiO<sub>x</sub> photoanode for 50 h at 1.23 V<sub>RHE</sub> in comparison with Ta:Fe<sub>2</sub>O<sub>3</sub> photoanode. Reprinted with permission from ref.27. Copyright 2023 American Chemical Society.



**Supplementary Fig. 9** Schematic synthesis procedure of Ta:Fe<sub>2</sub>O<sub>3</sub>@Fe<sub>2</sub>O<sub>3</sub> homojunction nanorods. Reprinted with permission from ref.28. Copyright 2020 Springer Nature.

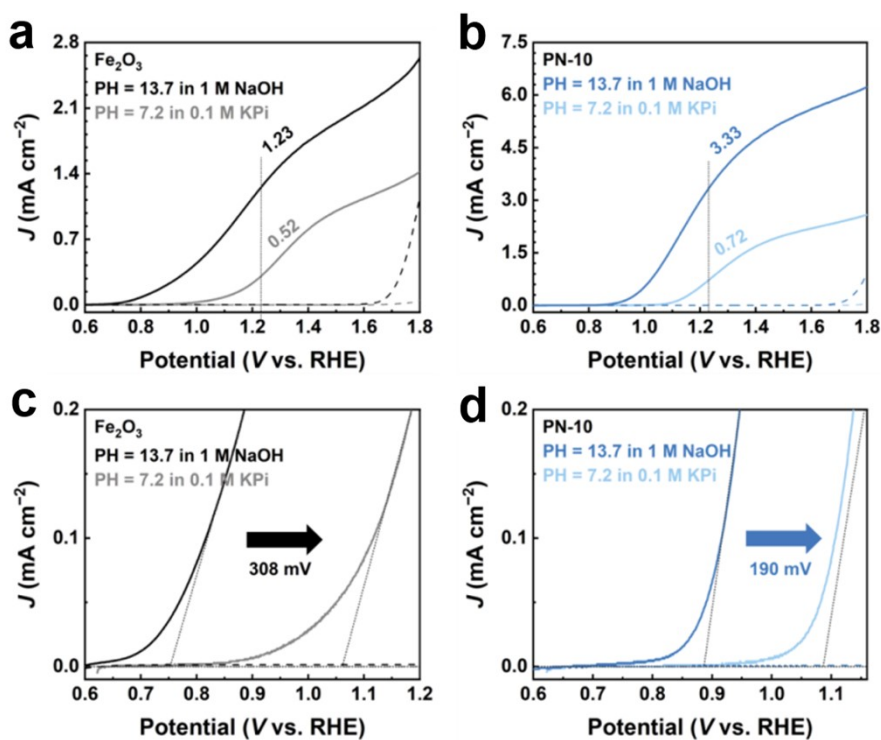


**Figure S10.** J–V curves of bare Fe<sub>2</sub>O<sub>3</sub> (a, c) and PN-10 (b, d) in alkaline (pH 13.7) and near-neutral (pH 7.2) electrolytes. Reprinted with permission from ref.29. Copyright 2024 Springer Nature.